

149  
NASA TM X-

66028

X-553-72-273

PREPRINT

# DEFORMATION AND INSTABILITY OF UNDERTHRUSTING LITHOSPHERIC PLATES

HAN-SHOU LIU

(NASA-TM-X-66028) DEFORMATION AND  
INSTABILITY OF UNDERTHRUSTING LITHOSPHERIC  
PLATES H. Liu (NASA) Aug. 1972 19 p CSCL

08K

N72-32397

Unclas

G3/13 41746

AUGUST 1972



— GODDARD SPACE FLIGHT CENTER —  
GREENBELT, MARYLAND

Paper presented at The International Union of Geophysics and Geodesy —  
9th Annual Symposium on Geophysical Theory and Computers, Banff,  
Canada, August 24-31, 1972.

Reproduced by  
NATIONAL TECHNICAL  
INFORMATION SERVICE  
U S Department of Commerce  
Springfield VA 22151

DEFORMATION AND INSTABILITY  
OF UNDERTHRUSTING LITHOSPHERIC PLATES

Han-Shou Liu

Geodynamics Branch

Trajectory Analysis and Geodynamics Division

August 1972

Paper presented at The International Union of Geophysics and Geodesy - 9th Annual Symposium on Geophysical Theory and Computers, Banff, Canada, August 24-31, 1972.

GODDARD SPACE FLIGHT CENTER

Greenbelt, Maryland

DEFORMATION AND INSTABILITY  
OF UNDERTHRUSTING LITHOSPHERIC PLATES

ABSTRACT

Recent confirmation of the relationship between seismology and tectonic plate movement has focused attention on the deformation and instability of lithospheric plates. In this paper we construct models of the underthrusting lithosphere for the calculation of displacement and deflection. The first of our three contributions is a mathematical theory that rigorously demonstrates the elastic instability in the descending lithosphere. The theory states that lithospheric thrust beneath island arcs becomes unstable and suffers deflection as the compression increases. Thus, in the neighborhood of the edges where the lithospheric plate plunges into the asthenosphere and mesosphere its shape will be contorted. The second contribution is our calculation of the lateral displacement. We show that, before contortion, the plate will thicken and contract at different positions with the variation in thickness following a parabolic profile. Finally, we explain the depth distribution of the intermediate and deep focus earthquakes in terms of plate buckling and contortion.

PRECEDING PAGE BLANK NOT FILMED

**Preceding page blank**

## CONTENTS

	<u>Page</u>
ABSTRACT . . . . .	iii
INTRODUCTION . . . . .	1
STRAIN ENERGY . . . . .	2
CONTORTION . . . . .	3
LATERAL DISPLACEMENT . . . . .	6
CONCLUSION . . . . .	9
REFERENCES . . . . .	9

PRECEDING PAGE BLANK NOT FILMED

Preceding page blank

# DEFORMATION AND INSTABILITY OF UNDERTHRUSTING LITHOSPHERIC PLATES

## INTRODUCTION

The inclined zones of seismicity which characterize all active island-arc systems are curved along their length. For some cases they can be recognized down to about 600 km. Since most arcs exhibit a more or less well-defined zone of maximum and minimum in seismic activity in the mantle, it is reasonable to ask whether such features of seismic activities are associated with the deformation and instability of the sinking lithosphere (Isacks, Oliver and Sykes, 1968; Roman, 1970). In this paper, we shall investigate the regions of instability and analyze the patterns of deformation of the underthrusting lithospheric plates. The principal difficulty we meet, when the problem of deformation of an unstable plate is to be posed in its mechanical form, consists in the behavior of the plate material. In order to obtain the first approximation, we assume that the plate is brittle enough to produce earthquakes by local fracture and elastic to maintain its shape at a depth of 600 km after passing through perhaps 1000 km of mantle (Sykes, 1966; McKenzie, 1969). The other difficulty is of a mathematical nature and in order to find the solutions of the equations of the problem the simplest schemes and elementary methods of analysis are used. Solutions of the theory of plates are given in forms which facilitate the computation of bending, twisting, compression, contortion and displacement of the plate. For the present purpose, the thermal effect on the distortion of plate is neglected. We shall, also, discuss

the results of this analysis in comparison with the observed depth ranges (Fig. 1) of seismic activities.

## STRAIN ENERGY

We consider the plate element  $dx dy$  shown in Fig. 2 subjected to the bending moments  $M_x$ ,  $M_y$  and twisting moments  $M_{xy}$  and  $M_{yx}$ . The strain energy due to these moments is given by (Love, 1944; Timoshenko and Woinowsky-Krieger, 1959)

$$\begin{aligned} dU_1 = & \left( \frac{1}{2} M_x dy \right) \left( \frac{\partial^2 \eta}{\partial x^2} dx \right) + \left( \frac{1}{2} M_y dx \right) \left( \frac{\partial^2 \eta}{\partial y^2} dy \right) \\ & + \left( \frac{1}{2} M_{xy} dy \right) \left( - \frac{\partial^2 \eta}{\partial y \partial x} dx \right) + \left( \frac{1}{2} M_{yx} dx \right) \left( \frac{\partial^2 \eta}{\partial x \partial y} dy \right) \end{aligned} \quad (1)$$

where in each term the first bracket gives the average total moment on the element and the second gives the angle through which it acts.

The bending and twisting moments are defined by

$$\begin{aligned} M_x &= - \frac{Eh^3}{12(1-\mu^2)} \left( \frac{\partial^2 \eta}{\partial x^2} + \mu \frac{\partial^2 \eta}{\partial y^2} \right) \\ M_y &= - \frac{Eh^3}{12(1-\mu^2)} \left( \frac{\partial^2 \eta}{\partial y^2} + \mu \frac{\partial^2 \eta}{\partial x^2} \right) \\ M_{xy} &= \frac{Eh^3}{12(1-\mu^2)} (1-\mu) \frac{\partial^2 \eta}{\partial x \partial y} = - M_{yx} \end{aligned} \quad (2)$$

where  $E$  is the modulus of elasticity,  $h$  is the thickness of the plate,  $\mu$  is the Poisson's ratio and  $\eta$  is deflection.

By substituting equation (2) into equation (1), we obtain the expression of this energy stored in the plate in terms of the deformation pattern. This is

$$U_1 = \frac{1}{2}D \iint \left\{ \left( \frac{\partial^2 \eta}{\partial x^2} + \frac{\partial^2 \eta}{\partial y^2} \right)^2 - 2(1-\mu) \left[ \frac{\partial^2 \eta}{\partial x^2} \frac{\partial^2 \eta}{\partial y^2} - \left( \frac{\partial^2 \eta}{\partial x \partial y} \right)^2 \right] \right\} dx dy \quad (3)$$

where

$$D = \frac{Eh^3}{12(1-\mu^2)}$$

Since the underthrusting lithospheric plate cannot sink through the denser mantle, it is subjected to a buoyancy  $T$  from the mesosphere. The buoyancy  $T$  is a compression load. Therefore the strain energy in the center plane of the plate due to deformation in the  $z$  direction is

$$U_2 = \frac{1}{2} \iint T \left( \frac{\partial \eta}{\partial x} \right)^2 dx dy \quad (4)$$

Adding equations (3) and (4) gives the total energy in the plate due to bending strain, twisting strain and strains in the center plane of the plate

$$\begin{aligned} U &= U_1 + U_2 \\ &= \frac{1}{2}D \iint \left\{ \left( \frac{\partial^2 \eta}{\partial x^2} + \frac{\partial^2 \eta}{\partial y^2} \right)^2 - 2(1-\mu) \left[ \frac{\partial^2 \eta}{\partial x^2} \frac{\partial^2 \eta}{\partial y^2} - \left( \frac{\partial^2 \eta}{\partial x \partial y} \right)^2 \right] \right\} dx dy \\ &\quad + \frac{1}{2} \iint T \left( \frac{\partial \eta}{\partial x} \right)^2 dx dy \end{aligned} \quad (5)$$

Equation (5) will be used for the analysis of plate contortion.

## CONTORTION

The mode of plate contortion can be obtained by using the energy method. Let us consider a rectangular underthrusting lithospheric plate under bending,

twisting and compression. The three dimensions of the plate are  $a$ ,  $b$  and  $h$  as shown in Fig. 3a. A resultant component  $p$  of the forces due to thermal convection in the mantle (Fig. 3b) is assumed to act at  $(\xi, \zeta)$ . Assuming simple support on the edges of the plate in the mesosphere and lithosphere makes it possible to choose a deflection in the form (Timoshenko and Woinowsky-Krieger, 1959)

$$\eta = \sum_{m=1}^{\infty} \sum_{n=1}^{\infty} A_{mn} \sin \frac{m\pi x}{a} \sin \frac{n\pi y}{b} \quad (6)$$

Substitution of equation (6) into equation (5) yields

$$U = \frac{\pi^4 ab}{8} D \sum_m \sum_n A_{mn}^2 \left( \frac{m^2}{a^2} + \frac{n^2}{b^2} \right)^2 + \frac{ab}{8} T \sum_m \sum_n A_{mn}^2 \left( \frac{m\pi}{a} \right)^2 \quad (7)$$

The change in potential energy due to  $p$  is equal to

$$W = p \sum_m \sum_n A_{mn} \sin \frac{m\pi \xi}{a} \sin \frac{n\pi \zeta}{b} \quad (8)$$

The total energy in the system must then be minimized with respect to the amplitude term  $A_{mn}$ , or

$$\frac{\partial (U - W)}{\partial A_{mn}} = 0 \quad (9)$$

By substituting equations (7) and (8) into equation (9), we have

$$\begin{aligned} \frac{\pi^4 ab}{4} D A_{mn} \left( \frac{m^2}{a^2} + \frac{n^2}{b^2} \right)^2 + \frac{ab}{4} A_{mn} T \left( \frac{m\pi}{a} \right)^2 \\ - p \sin \frac{m\pi \xi}{a} \sin \frac{n\pi \zeta}{b} = 0 \end{aligned} \quad (10)$$



from which

$$A_{mn} = \frac{4p \sin \frac{m\pi\xi}{a} \sin \frac{n\pi\zeta}{b}}{\pi^4 ab D \left[ \left( \frac{m^2}{a^2} + \frac{n^2}{b^2} \right)^2 + \frac{1}{\pi^2 D} \cdot \frac{m^2}{a^2} T \right]}. \quad (11)$$

Putting equation (11) into equation (6), the deflection equation is

$$\eta = \frac{4p}{\pi^4 ab D} \sum_m \sum_n \frac{\sin \frac{m\pi\xi}{a} \sin \frac{n\pi\zeta}{b}}{\left( \frac{m^2}{a^2} + \frac{n^2}{b^2} \right)^2 + \frac{1}{\pi^2 D} \frac{m^2}{a^2} T} \sin \frac{m\pi x}{a} \sin \frac{n\pi y}{b} \quad (12)$$

In equation (12),  $T$  is a compression load, its sign will be negative and the value of this negative term may become great enough so that the denominator of equations (11) and (12) approaches zero. Under these circumstances, the deflection  $\eta$  approaches a very large value irrespective of how small the normal force  $p$  may be. A possible mode of plate contortion for  $m = 2$  and  $n = 1$  is shown in Fig. 4. In Fig. 4, A and B are regions of maximum curvature and C is the neutral position.  $T$  will increase when the plate continues to thrust into the mesosphere. As  $T$  increases to a value such that the stresses in the plate approach their critical value, buckling may occur in region A or B. No fracture will appear in the neutral region C in which the contortion of the plate changes sign. Therefore, the simplest explanation, one direct consequence of the model of Fig. 4, is that the intermediate maxima in seismic activity for island arcs are restricted to the regions of instability A and B in the asthenosphere. For the purpose of comparison, we have plotted the depth ranges of maxima in the seismic activity for several island arcs in Fig. 4. It shows clearly that the

depth ranges of maxima in seismic activity are correlated with the computed regions of instability. In a worldwide composite plot of seismic activity versus depth (Isacks, Oliver and Sykes, 1968), a minimum in activity appears near the depth of about 300 km. Thus, the existence of a neutral region in the underthrusting lithospheric plates seems to provide a geophysical explanation for the absence of seismic activity at this depth.

### LATERAL DISPLACEMENT

In order to compute the lateral displacement, we consider a plate which is dragged against the mesosphere because of convection. To simplify the problem we assume that the deformation of the plate corresponds to a plane strain before contortion occurs. Fig. 5 represents an underthrusting lithospheric plate with thickness  $h$  and width  $b$ . The strain is considered in the  $xz$  plane. The components of displacement  $u$  and  $v$  of a point in the plate are the solutions of the following equations (Love, 1944; Timoshenko and Woinowsky-Krieger, 1959)

$$\begin{aligned} \left( \frac{\partial^2}{\partial x^2} + \frac{\partial^2}{\partial z^2} \right) u + \frac{\lambda + G}{G} \left( \frac{\partial^2 u}{\partial x^2} + \frac{\partial^2 v}{\partial x \partial z} \right) &= 0 \\ \left( \frac{\partial^2}{\partial x^2} + \frac{\partial^2}{\partial z^2} \right) v + \frac{\lambda + G}{G} \left( \frac{\partial^2 u}{\partial x \partial z} + \frac{\partial^2 v}{\partial z^2} \right) &= 0 \end{aligned} \tag{13}$$

where

$$\lambda = \frac{\mu E}{(1 + \mu)(1 - 2\mu)}$$

and  $G$  is the modulus of rigidity. In equation (13), body forces are neglected.

Differentiating these equations, the first with respect to  $x$ , the second with respect to  $z$ , and adding them together, we find

$$\left( \frac{\partial^2}{\partial x^2} + \frac{\partial^2}{\partial z^2} \right) \left( \frac{\partial u}{\partial x} + \frac{\partial v}{\partial z} \right) = 0. \quad (14)$$

Therefore, the volume expansion  $\frac{\partial u}{\partial x} + \frac{\partial v}{\partial z}$  satisfies the Laplace equation.

The solutions of equations (13) are

$$u = - \frac{\lambda + G}{2G} x \left( \frac{\partial u}{\partial x} + \frac{\partial v}{\partial z} \right) + \phi_1 \quad (15)$$

$$v = - \frac{\lambda + G}{2G} z \left( \frac{\partial u}{\partial x} + \frac{\partial v}{\partial z} \right) + \phi_2$$

where  $\phi_1$  and  $\phi_2$  are harmonic, i.e.,

$$\begin{aligned} \left( \frac{\partial^2}{\partial x^2} + \frac{\partial^2}{\partial z^2} \right) \phi_1 &= 0 \\ \left( \frac{\partial^2}{\partial x^2} + \frac{\partial^2}{\partial z^2} \right) \phi_2 &= 0. \end{aligned} \quad (16)$$

The general solutions of equations (14) and (16) can be expressed in the following forms

$$\begin{aligned} \frac{\partial u}{\partial x} + \frac{\partial v}{\partial z} &= A_0 + \sum_{k=1}^{\infty} [A_k (x + iz)^k + B_k (x - iz)^k] \\ \phi_1 &= C_0 + \sum_{k=1}^{\infty} [C_k (x + iz)^k + D_k (x - iz)^k] \\ \phi_2 &= E_0 + \sum_{k=1}^{\infty} [E_k (x + iz)^k + F_k (x - iz)^k] \end{aligned} \quad (17)$$

where the coefficients  $A_0$ ,  $C_0$ ,  $E_0$ ,  $A_k$ ,  $B_k$ ,  $C_k$ ,  $D_k$ ,  $E_k$  and  $F_k$  are to be determined by the stresses on the boundary of the plate. The stress-displacement

relationships are

$$\begin{aligned}
\sigma_{xx} &= \lambda \left( \frac{\partial u}{\partial x} + \frac{\partial v}{\partial z} \right) + 2G \frac{\partial u}{\partial x} \\
\sigma_{xz} &= G \left( \frac{\partial u}{\partial x} + \frac{\partial v}{\partial z} \right) \\
\sigma_{zz} &= \lambda \left( \frac{\partial u}{\partial x} + \frac{\partial v}{\partial z} \right) + 2G \frac{\partial v}{\partial z}
\end{aligned} \tag{18}$$

By prescribing  $\sigma_{xx}$ ,  $\sigma_{xz}$  and  $\sigma_{zz}$  on the plate boundary, we obtain the vertical displacement  $v$  in equation (15) on the surface of the plate for  $\frac{x^2}{b^2} \ll 1$ .

$$v = \pm \frac{\lambda}{2G(\lambda + G)} \left[ x^2 - \left( \frac{b^2}{16} + \frac{3\lambda + 2G}{48\lambda} h^2 \right) \right] \quad T \tag{19}$$

Equation (19) shows that the plate, being thickened for small values of  $x$ , may form symmetrical buckles on both surfaces  $z = \pm h/2$ . The displacement  $v$  vanishes for

$$x = x_0 = \frac{1}{4} \left( b^2 + \frac{3\lambda + 2G}{3\lambda} h^2 \right)^{1/2} \tag{20}$$

For  $x > x_0$ ,  $v$  changes sign. That is, in this region, the plate begins to be contracted. This region corresponds to a phase change in the material (Anderson, 1967). Therefore, the leading parts of the underthrusting lithospheric plates may be deformed with a parabolic profile and the buckling in this unstable region seems to be the cause of the deep seismic activities (Fig. 5). It should be noted that, if we take into account the real case of boundary conditions and the effects of thermal stresses and body forces on the distortion of plate, there will be no symmetry with respect to the axis  $x$  or the buckling. However, it may be expected that the plate will show a tendency to contort as a whole and to thicken in the mesosphere.

## CONCLUSION

We have developed mathematical models of the underthrusting lithospheric plates to determine the regions of instability and to compute the patterns of deformation. Two types of plate buckling in the asthenosphere and mesosphere are discussed. The absence of seismological events at the depth of 300 km is explained in terms of the mode of plate contortion. In comparison with the worldwide composite plot of seismic activity versus depth, we conclude that the deep and intermediate – depth earthquakes are restricted to those regions of instability in which buckling of the plate may occur.

## REFERENCES

- Anderson, D. L., Phase Changes in the Upper Mantle, *Science*, 157, 1165, 1967.
- Gutenberg, B., and C. F. Richter, *Seismicity of the Earth*, Princeton University Press, Princeton, N.J., 1954.
- Isacks, B., J. Oliver, and L. R. Sykes, *Seismology and the New Global Tectonics*, *J. Geophys. Res.*, 73, 5855, 1968
- Love, A. E. H., *A Treatise on the Mathematical Theory of Elasticity*, Dover Publication, New York, 1944.
- McKenzie, D. P., *Speculations on the Consequences and Causes of Plate Motions*, *Geophys. J.*, 18, 1, 1969.

Roman, C. , Seismicity in Romania — Evidence for the Sinking Lithosphere,  
Nature, 228, 1176, 1970.

Sykes, L. R. , The Seismicity and Deep Structure of Island Arcs, J. Geophys.  
Res. , 71, 2981, 1966.

Timoshenko, S. , and S. Woinowsky-Krieger, Theory of Plates and Shells,  
McGraw-Hill Inc. , New York, 1959.

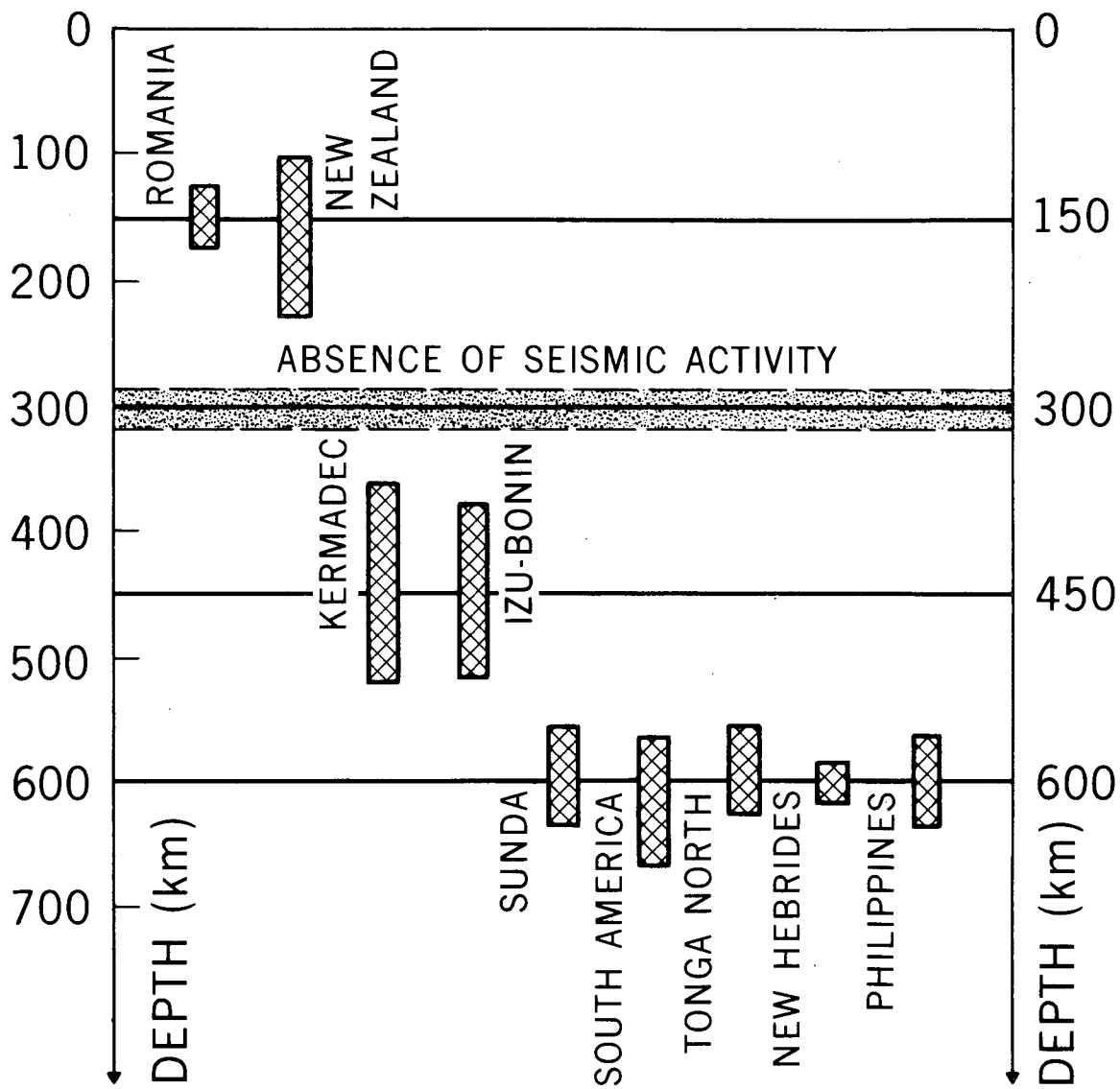


Figure 1. Worldwide composite plot of seismic activity versus depth. The data are from Gutenberg and Richter (1954), Sykes (1966), Isacks, Oliver and Sykes (1968) and U. S. Coast and Geodetic Survey.

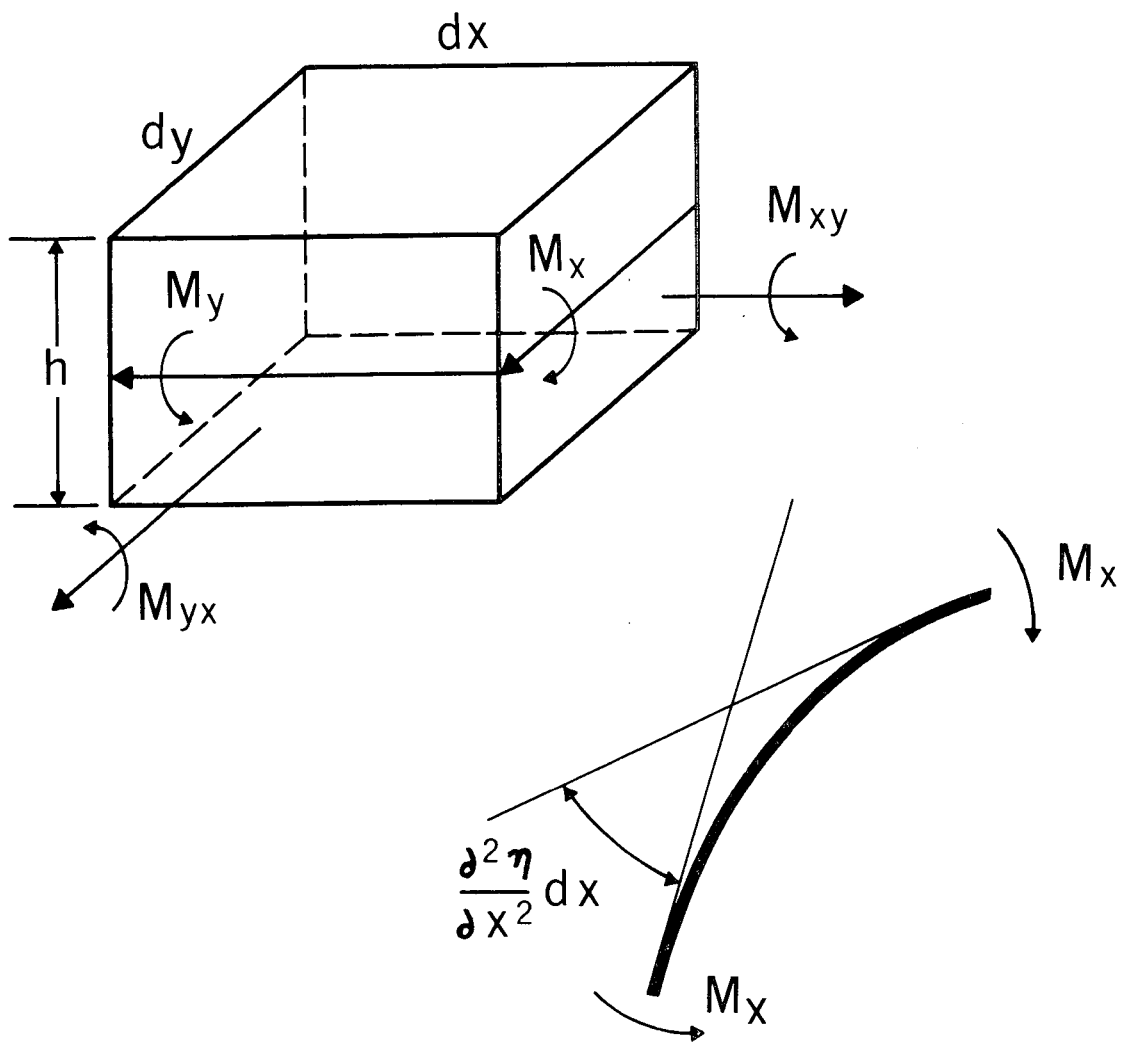


Figure 2. Plate element.



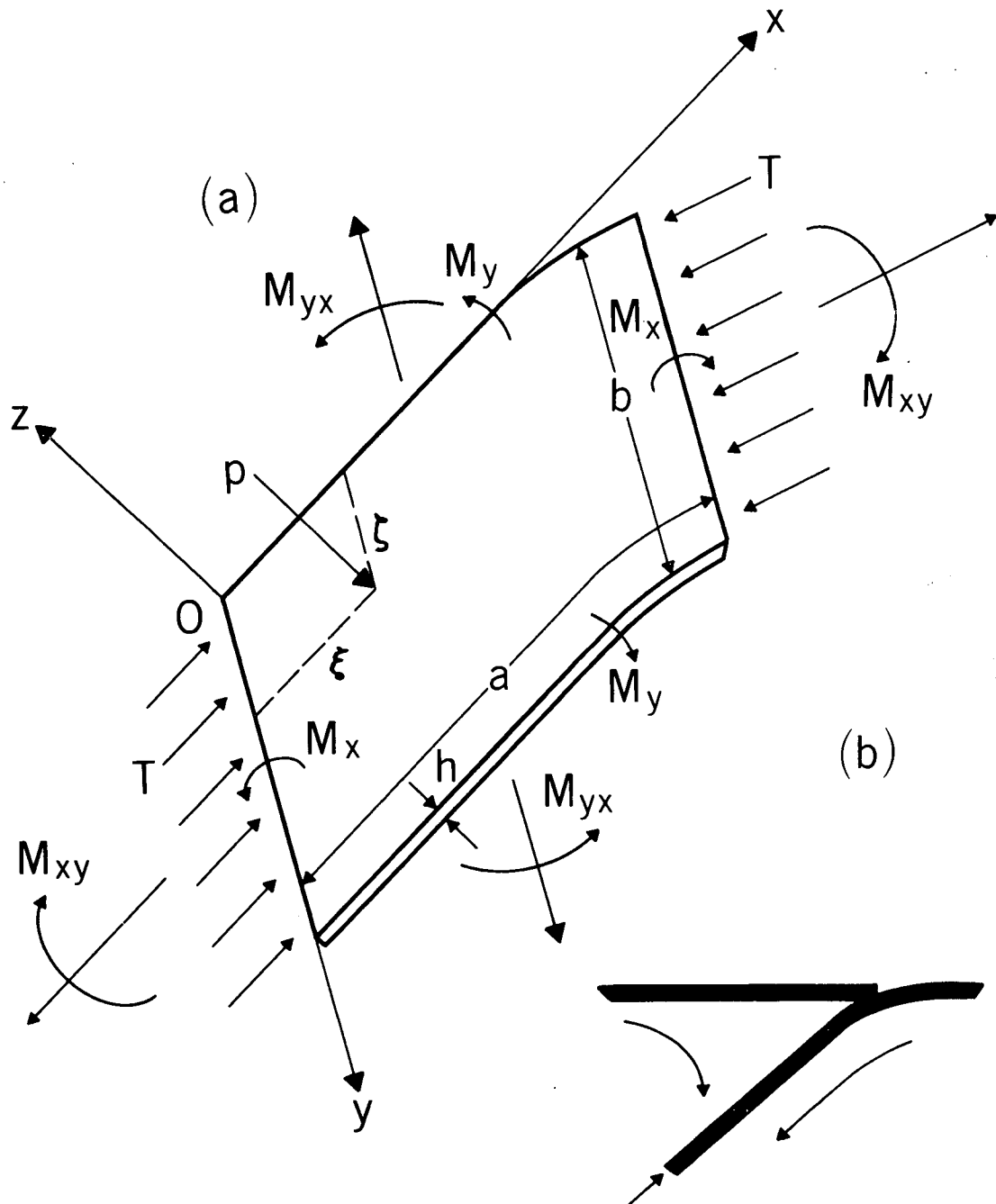


Figure 3. (a) Plate under bend, twist and compression. A resultant component  $p$  of the convection force in the mantle on both sides of the plate acts at  $(\xi, \zeta)$ . (b) Underthrusting lithospheric plate is subjected to normal forces in convection cells.

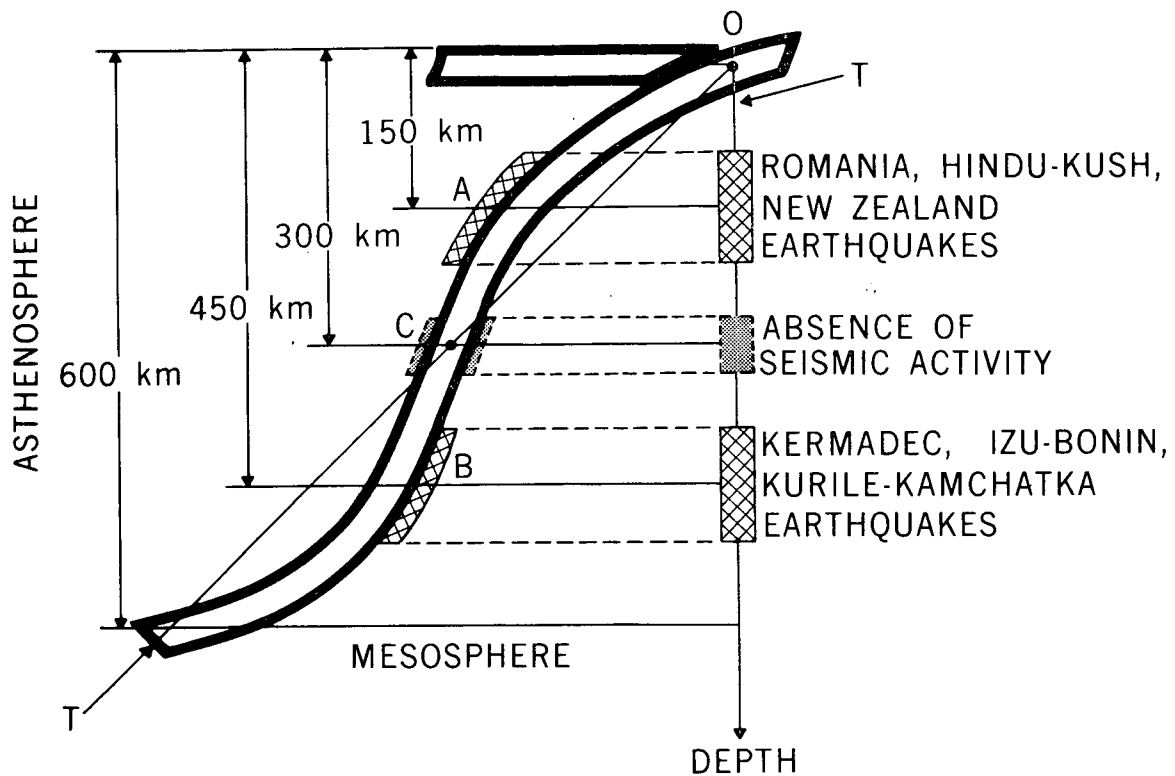


Figure 4. Mode of plate contortion and the depth ranges of intermediate maxima in seismic activities for several island arcs. The neutral region C of the plate corresponds to the depth of minimum in seismic activity. A and B are regions of instability in asthenosphere.

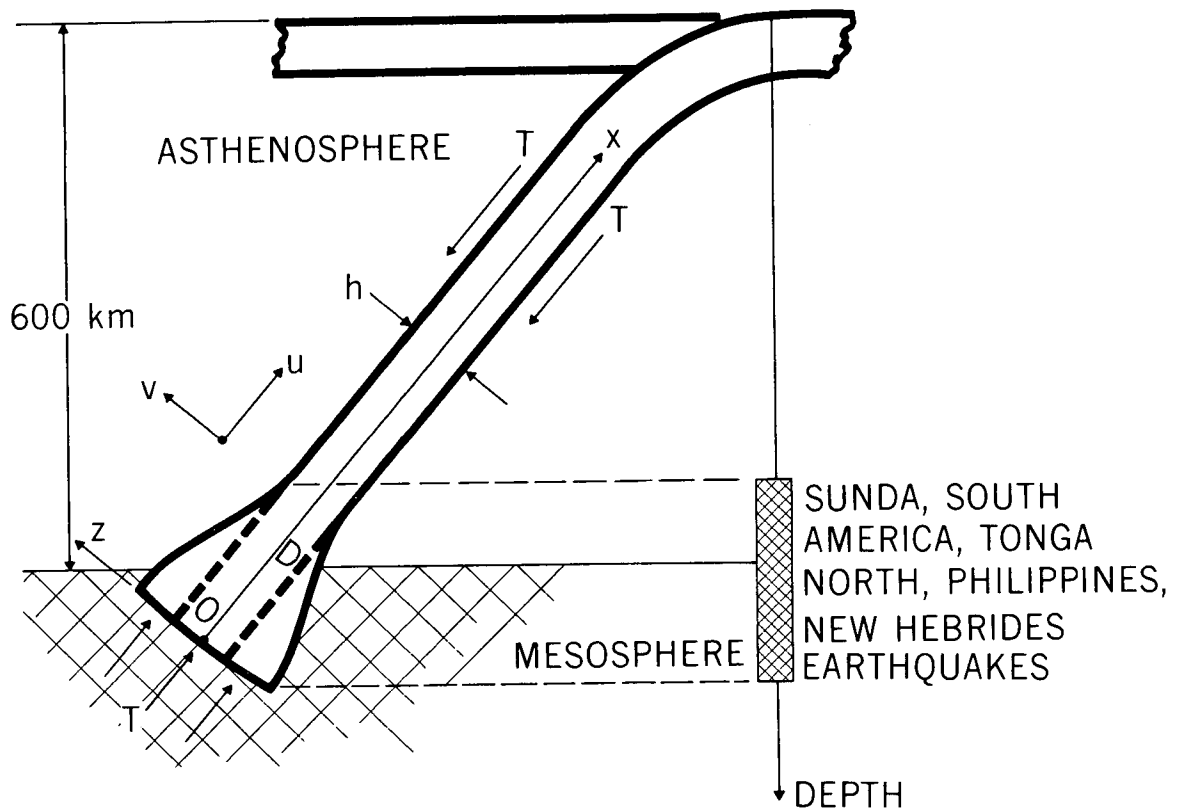


Figure 5. Plate buckling in mesosphere and the depth range of deep maxima in seismic activities for several island arcs. The leading part D of the plate is the region of instability near the boundary of mesosphere and asthenosphere.